Strongly Modified Reflection Contrast of Semiconductor Nanowires by Nanoshells

Silke L Diedenhofen[1], Rienk E Algra[2,3,4], Erik P A M Bakkers[2,5,6] and Jaime Gómez Rivas[1,5]

[1] FOM Institute AMOLF, c/o Philips Research Laboratories Eindhoven, High Tech Campus 4, 5656 AE Eindhoven, The Netherlands
[2] Philips Research Laboratories Eindhoven, 5656 AE Eindhoven, The Netherlands
[3] Materials innovation institute (M2i), 2628 CD Delft, The Netherlands
[4] IMM, Solid State Chemistry, Radboud University Nijmegen, Heyendaalseweg 135, 6525 AJ Nijmegen, The Netherlands
[5] Applied Physics, Photonics & Semiconductor Nanophysics, Eindhoven University of Technology, 5600 MB Eindhoven, The Netherlands
[6] Kavli Institute of Nanoscience, Quantum Transport, Delft University of Technology, 2600 GA Delft, The Netherlands

E-mail: `rivas@amolf.nl`

Abstract. The propagation of light in dense ensembles of vertically aligned nanowires is determined by their unique and extreme optical constants. Depending on the nanowire filling fraction and their diameter, layers of nanowires form a strongly birefringent medium. This large birefringence gives rise to extremely sharp angle dependent resonances in polarized reflection with full-widths at half-maximum narrower than 1°. These resonances are very sensitive to small changes in the medium surrounding the nanowires. We demonstrate experimentally the tunability of the reflection resonances from ensembles of nanowires due to changes in their surrounding by adding shells of SiO_2 with thicknesses ranging from 10 nm to 30 nm around the nanowires. We model the modification of the reflection with Maxwell-Garnett effective medium theory and Jones Calculus for anisotropic layers. The strong modification of these resonances renders nanowire ensembles a promising candidate for sensing applications with a high sensitivity to molecular thin layers.

PACS numbers: 78.40.Fy, 78.67.Uh

Submitted to: *Nanotechnology*

1. Introduction

Recent progress in nanofabrication technology has opened new avenues in research on semiconductor nanowires. The high control of nanowire dimensions [1], shape [2], and position [3, 4] as well as direction [5]; and the growth of radial and axial homo- and hetero-junctions [6, 7] results in novel effective media with unique and extreme optical properties. Nanowire layers have been demonstrated as broadband and omni-directional antireflection layers [8, 9], as photosensitive devices [10, 11], and as optical cloaks due to exact positioning of tapered nanowires. [3] The large aspect ratio of nanowires, i.e., the large difference between their diameter and length, results in a large optical anisotropy.[12, 13] Giant form birefringence has been reported in dense ensembles of aligned nanowires [14], i.e., light propagating in a nanowire layer is refracted differently depending on its polarization. A direct consequence of the giant birefringence is a resonance in the reflection contrast.[15, 16] This contrast is defined as the light reflected from a birefringent layer transmitted through a polarizer and analyzer set in a crossed configuration, normalized to the reflection of the same layer measured with parallel aligned polarizer and analyzer.

Here, we demonstrate experimentally that the narrow resonances in the reflection contrast of birefringent ensembles of nanowires can be tuned by changing the medium surrounding the nanowires. Specifically, we determine a large shift of the reflection contrast as a function of angle of incidence by coating the nanowires with SiO_2 shells with different thicknesses. We find that shells as thin as 10 nm significantly modify the reflection contrast, and we model this modification using Maxwell-Garnett effective medium theory for coated cylinders [17] and Jones calculus.[18] The large sensitivity of the reflection contrast to changes in the surroundings of the nanowires is quantified. Our results demonstrate that ensembles of nanowires constitute an alternative to porous media for optical sensing. Porous media are very sensitive to changes in their surroundings because of their large surface to volume ratio.[15, 19–23] A modification of reflection [19] and transmission [15] as well as birefringence [20] has been demonstrated in porous silicon by infiltrating the pores with DNA [21], proteins [22], or gases [23]. In principle, all these sensors have one thing in common, namely, they detect a change in the refractive index of the material filling the pores. The very open structure of nanowire samples compared to porous media, facilitates the infiltration of the layer, which may constitute an important advantage of nanowire based sensors.

2. Nanowire Growth and Shell Deposition

We have grown dense ensembles of GaP nanowires on a GaP substrate using the vapor-liquid-solid growth mechanism [24] by metal-organic vapor phase epitaxy using trimethyl-gallium (TMG) and phosphine (PH_3) as precursors. The VLS growth mechanism requires a metal catalyst particle. To achieve dense ensembles of vertically aligned nanowires, we have deposited gold by electron beam evaporation such that an

equivalent layer thickness of 0.3 nm is achieved. The nanowires are grown in the MOVPE reactor during 1080 s using the VLS growth mechanism at a temperature of 420 °C and during 200 s in a lateral growth mode at 630 °C to increase the filling fraction of GaP in the layer. Figure 1a shows a cross-sectional scanning electron micrograph (SEM) of the nanowire layer. From Figure 1a and similar SEM images we have determined the thickness of the nanowire layer to be 1 ± 0.1 μm. We have also determined the diameter distribution of the nanowires, which is given in the histogram of Figure 1b. The average nanowire diameter is 33 ± 9 nm. From top-view SEM images (Figure 1c), we observe that the nanowires cluster together. Due to the clustering, the average distance between nanowires is difficult to determine, though we can estimate it to be on the order of 100 to 200 nm.

To determine the modification of the reflection from nanowire layers to small changes in the surrounding, we have coated several samples with SiO_2 shells of different thicknesses. Therefore, we cleaved the sample into five pieces. SiO_2 was evaporated on four pieces by plasma-enhanced chemical vapor deposition (PECVD) at a temperature of 300 °C and a pressure of 2.4 Torr for 4 s, 8 s, 15 s, and 20 s. The fifth sample was left unchanged as a reference.

We have determined the SiO_2 shell thicknesses by transmission electron microscopy (TEM). Figure 1d shows a TEM image of a GaP nanowire with a core diameter of 15 ± 1 nm coated with SiO_2 with a shell thickness of 28 ± 2 nm. It is remarkable that the SiO_2 shell has a constant thickness over the nanowire length, which indicates a good infiltration of the nanowire layer during the PECVD. The core of the nanowire contains defects, which we determined to be twin planes perpendicular to the growth direction. The gold particle used to catalyze the growth of the wires is visible on top of the nanowire. Both the twin planes and the gold particle have no significant effect on the optical properties discussed next [14, 16]. Table 1 gives the evaporation times and the resulting shell thicknesses around the nanowires.

3. Results and Discussion

Dense ensembles of nanowires such as the sample displayed in Figure 1 form strongly birefringent media with an ordinary, n_o, and an extraordinary, n_e, refractive index for light polarized perpendicular and parallel to the nanowire axis, respectively.[14] The birefringence of the nanowire layer results in narrow resonances in the reflection contrast, as it is described below. We have measured the angularly resolved reflection contrast using linearly polarized incident light with a wavelength of 532 nm. Therefore, the nanowire sample and the detector are mounted on two computer controlled rotational stages that allow θ-2θ measurements. In this setup the sample and the detector can be rotated. This rotation varies the angle of incidence onto the sample θ. The detector is rotated around the the sample to an angle 2θ to measure the specular reflection. The incident polarization is set to 45° with respect to the plane of incidence in order to have an equal intensity for s- and p-polarized light. Two measurements are

performed to determine the reflection contrast: One with the analyzer aligned nearly parallel, $I_{\parallel}$, and the other with the analyzer aligned nearly perpendicular, $I_{\perp}$, to the incident polarization. To increase the amplitude of the reflection contrast, the analyzer is optimized to achieve a minimum intensity for parallel alignment and a maximum intensity for crossed alignment. A schematic of the experimental setup is given in Figure 2a. This figure displays the polarization vector, the angle of incidence, and the orientation of the nanowires with respect to the incident light. For clarity, the nanowires are represented as a periodic array. The sample, however, is formed by a random ensemble of GaP nanowires.

We have measured the reflection contrast on the uncoated nanowire sample (Sample I in Table 1) as a function of angle of incidence using a beam size of less than 1 mm on the sample. Figure 3a shows these measurements (black squares). The reflection contrast has a maximum of 2450 at an angle of 53.99° and a full-width at half maximum (FWHM) of 0.63°. This pronounced maximum is due to the birefringence of the nanowire layer and can be explained as follows. Figure 2b schematically describes the propagation of linearly polarized light in the nanowire layer. Linearly polarized light with arbitrary polarization can be expressed as a superposition of s- and p-polarized light. Therefore, the incident light with a polarization at an angle of 45° with respect to the plane of incidence (purple line in Figure 2b) can be split into two components: Light with the electric field component perpendicular to the nanowire elongation travels as a s-polarized wave in the layer (blue line in Figure 2b), while light with the electric field component parallel to the nanowire elongation travels as a p-polarized wave (red line in Figure 2b). The s-polarized wave refracts into the nanowire layer according to the refractive index n_{s}, while the p-polarized wave is refracted according to n_{p}. The effective refractive indices for s- and p-polarization can be derived from the ordinary and extraordinary refractive indices of the nanowire layer. For s-polarization, the electric field is perpendicular to the long axis of the nanowires for any angle of incidence. Therefore, the refractive index for s-polarization equals the ordinary refractive index, $n_{\mathrm{s}} = n_{\mathrm{o}}$.[25] For normal incidence, the electric field is perpendicular to the nanowire axis for both polarizations. As the angle of incidence onto the sample is varied, the effective refractive index for p-polarized light increases due to the larger projection of the electric field vector along the nanowire axis.[26] The difference between n_{s} and n_{p} introduces a phase shift between s- and p-polarized light while traveling through the nanowire layer. This phase shift depends on the layer thickness L, the vacuum wavelength λ, the refractive indices $n_{\mathrm{s,p}}$, and the internal angles of propagation $\theta_{\mathrm{s,p}}$ for s- and p-polarization, respectively, which are related to the angle of incidence by Snell's law. The phase shift is given by [15]

$$\Delta\phi = \frac{4\pi}{\lambda} L(n_{\mathrm{p}} \cos\theta_{\mathrm{p}} - n_{\mathrm{s}} \cos\theta_{\mathrm{s}}). \tag{1}$$

If this phase shift equals π, the nanowire layer forms a $\lambda/2$-plate and the polarization is rotated by 90°, resulting in a maximum of $I_{\perp}$ and a concomitant minimum of $I_{\parallel}$. The reflection contrast in this case is maximum. As the reflection coefficient at the air-nanowire interface r_{nw} (see Figure 2b) depends on polarization, i.e., the intensity of

the reflected s-polarized wave is different than the reflected intensity of the p-polarized wave, the resulting polarization of the superposition of the reflected light with both components is not exactly rotated by 90°. To compensate for this effect, we optimize the analyzer for measuring a minimum in $I_{\parallel}$ and a maximum in $I_{\perp}$.

We have modeled the reflection contrast using Maxwell-Garnett effective medium theory for coated cylinders [17] and Jones calculus.[18] A detailed description of the calculation is given in Ref. 27 and in the Appendix. The core radius and permittivity, and the distance between the nanowires needs to be defined for calculating the reflection contrast. While the average core radius can be determined from the diameter distribution (Figure 1b) to be 16.5 ± 4.5 nm, the distance between the nanowires determined from top-view SEM images (Figure 1c) has a large uncertainty with a value between 100 and 200 nm. Therefore, the distance between the nanowires is used as a fitting parameter as well as the core radius within the range of core radii determined from SEM. The refractive index of the nanowire core is that of GaP at 532 nm (n = 3.5 + 0.0005i). [28] In Figure 3a, a fit to the measurement for the uncoated nanowires is included (red curve). The core radius of the nanowires obtained from this fit is r_{c} = 19.7 ± 1.0 nm and the distance between the nanowires d_{nw} = 160 ± 10 nm. The nanowire layer thickness is fixed to 1 μm in this fit. The angle formed by the optical axis of the analyzer and the incident polarization is set such that the amplitude of the calculated reflection contrast fits the amplitude of the measurement. From this fit, the birefringence paramenter $\Delta n = n_{\mathrm{e}} - n_{\mathrm{o}}$, with n_{e} and n_{o} being the extraordinary and the ordinary refractive index of the nanowire layer, respectively, is determined to be 0.19 ± 0.1.

To demonstrate the high sensitivity of the reflection contrast to changes in the nanowire dimensions, Figure 3b shows a calculation of this contrast for three different radii of nanowires, namely, 19.6 nm (black curve), 19.7 nm (red curve), and 19.8 nm (blue curve). A difference of 0.2 nm in the radius of the nanowires leads to an angular shift from 54.04° to 53.76°. The shift of the reflection contrast can be explained with Equation 1; as n_{p} and n_{s} depend on the GaP filling fraction in the nanowire layer, a phase shift of π between the s- and p-polarized wave is achieved at a different angle of incidence as the GaP filling fraction, thus the nanowire radius, is increased. Importantly, the reflection contrast decreases at 53.76° from 3009 to 1380 due to a reduction of the nanowire radius of 0.2 nm. This large decrease of the reflection contrast can allow the detection of mono-atomic layers.

The high sensitivity of the reflection contrast of nanowire layers to sub-nanometer variations in the nanowire radius renders these structures very interesting as ultrasensitive sensor to small dielectric changes in the surroundings of the nanowires. To demonstrate the sensitivity of the reflection contrast to these changes, we have calculated the reflection contrast of layers of GaP nanowires coated with thin shells of refractive index 1.45. This refractive index corresponds to that of SiO_2 at 532 nm,[28] and it is similar to the refractive index of biomolecules.[29] Figure 3c shows calculations of the reflection contrast at λ = 532 nm for nanowires without (black solid curve) and

with shells with thicknesses of 5 nm (red long-dashed curve), 10 nm (blue short-dashed curve), 15 nm (olive dash-dotted curve), and 30 nm (magenta dash-dot-dotted curve). The reference sample without a SiO_2 shell corresponds to the calculation fitting the measurement of Figure 3a. With increasing shell thickness, the reflection contrast peak shifts to larger angles of incidence. A SiO_2 shell of 5 nm shifts the reflection contrast by 0.8°. While increasing the GaP filling fraction results in a shift of the reflection contrast to smaller angles of incidence, adding a shell of SiO_2 around the nanowires shifts the reflection contrast to larger angles of incidence. This difference in the shift of the reflection contrast can be attributed to a different increase of n_s and n_p when adding a shell with a certain refractive index around the nanowires. The positive shift of the angle of the maximum reflection contrast is due to a larger increase of n_s than that of n_p with thicker shells (see Equation 1) [27]. Intriguingly, adding a shell of SiO_2 with a thickness of 5 nm around the nanowires does not only shift the reflection contrast by 0.8°, it also results in a decrease from 2250 to 450 at 53.99°. This strong decrease in reflection contrast could be easily detectable and does not require a rotation of the sample and detector.

To get a better understanding of the positive and negative shifts of the angle of maximum reflection contrast, depending on the refractive index of the shell, we have calculated the phase shift according to Equation 1 of light passing through a nanowires layer with a thickness of 1 μm. The nanowires have a radius of 19.65 nm, and the distance between them is 160 nm. Figures 3d and e display calculations of the phase shift as a function of angle of incidence and the GaP shell thickness, i.e., an increase in the nanowire radius (Figure 3d) or as a function of SiO_2 shell thickness (Figure 3e). The angle of incidence at which $\Delta\phi = \pi$ decreases, when increasing the nanowire radius by up to 20 nm. For a larger increase in the nanowire radius, this angle shifts to larger values. For SiO_2 shells, the phase shift shows a different behavior. The angle of incidence at which $\Delta\phi = \pi$ increases already for very thin layers when the shell thickness increases. The different behavior of the phase shift by increasing the radius and shell thickness with various materials can be explained by a different increase of n_s and n_p with increasing material volume fraction.

The calculations displayed in Figure 3b show a large sensitivity of the reflection contrast to changes in the diameter of the nanowires. Inhomogeneities on the sample will also give rise to shifts in the reflection contrast maximum. Therefore, we have measured the reflection contrast of the five samples coated with SiO_2 shells using an incident beam with a diameter of 2 mm. By using a large beam diameter, the reflection contrast is measured over a larger sample area and so are the inhomogeneities averaged. This averaging also reduces the angular resolution of the measurement. In this way, we can achieve a high reproducibility of the measurements and we can compare the reflection of the different samples. Figure 4a shows the measured reflection contrast of the five samples. The maximum reflection contrast of the uncoated nanowire sample is 162 and the FWHM is 1.8° (black squares). The FWHM of the reflection contrast peak in this measurement is broadened and the maximum is reduced with respect to the

measurement with an optical beam diameter of less than 1 mm due to a reduction of the resolution and the smearing of the reflection contrast resonance due to inhomogeneities in the sample. The measured reflection contrast from the layers of nanowires coated with SiO_2 are also displayed in Figure 4a for shell thicknesses of 10.3 ± 1.3 nm (red circles), 16.7 ± 2 nm (blue up-triangles), 18.6 ± 1.1 nm (olive down-triangles) and 29.3 ± 4.7 nm (magenta diamonds). In agreement to Figure 3c, the maximum in reflection contrast shifts to larger angles of incidence with increasing shell thickness.

We have modeled the reflection contrast using the core radius, the average distance between the nanowires, the shell thickness, and angle of the polarizer as fitting parameters. Figure 4b shows the fit to the measurement for the uncoated nanowires (black curve). The core radius of the nanowires obtained from this fit is $r_c = 19.4 \pm 1$ nm and the distance between the nanowires is $d_{nw} = 160 \pm 10$ nm. These values of r_c and d_{nw} are in agreement with those determined from the reflection contrast measured with a smaller beam diameter. Calculations of the reflection contrast for core-shell nanowires with SiO_2 thicknesses of 9 ± 1 nm (red long-dashed curve), 18 ± 1 nm (blue short-dashed curve), 19.7 ± 1 nm (olive dash-dotted curve), and 30 ± 1 nm (magenta dash-dot-dotted curve) are included. In Figure 4b both measurements and calculations show that a SiO_2 shell with a thickness of $\sim$ 10 nm shifts the peak of the reflection contrast by $\sim 1^\circ$ (red circles and dashed curve). The agreement between measurement and calculation indicates that measuring the reflection contrast allows to accurately determine the thickness of the SiO_2 shell. The small discrepancy between the thicknesses of the shell determined by TEM and by the fits to the measurements can be attributed to minor inhomogeneities in the shell thickness due to the deposition technique.

To determine the sensitivity of the reflection contrast to changes in the medium surrounding the nanowires, we analyze the peak shift as a function of the product of $\Delta n \cdot t$, being Δn the difference in the refractive index of the shell and the surrounding medium, i.e., air, and t the shell thickness. Figure 5 shows the peak shift obtained from the measurements using an optical beam diameter of $\sim$ 2 mm (black symbols) and obtained from the calculations (red curve) assuming a small beam diameter. Intriguingly, the measured and calculated shift of the reflection contrast follow a parabolic dependence with similar slope, although the beam diameter in the measurement is larger than that assumed in the calculation. This similar shift of the reflection contrast obtained from the measurement using a large beam diameter and from the calculation using a small beam diameter shows that the shift of the reflection contrast maximum is a very robust quantity, independent of the optical beam diameter, and therewith of the angular resolution of the experimental setup. This robustness of the shift of the reflection contrast can be explained with Equation 1, where it depends only on the phase shift between the s- and p-polarized reflected waves.

We have determined from the calculations the sensitivity of the shift of the reflection contrast change, with the change shell coating of the nanowires, $\frac{d(\Delta\theta)}{d(\Delta n \cdot t)}$. The inset of Figure 5 displays the sensitivity as a function of $\Delta n \cdot t$. The sensitivity follows a straight line with a slope of $\sim 0.05\ ^\circ/(\mathrm{nm} \cdot \mathrm{RIU})$, where RIU is a refractive index unit. Higher

sensitivities are thus obtained with thicker shells of high index materials. The overall high sensitivity of the reflection contrast, which shifts this contrast on the order of 0.5° per nanometer of a shell with a refractive index difference of one from the surroundings, can be attributed to the large surface to volume ratio of nanowires that allows probing small changes in their surrounding. Therefore, layers of nanowires are rendered as promising optical sensors.

4. Conclusion

In conclusion, we have demonstrated that the reflection contrast measured on layers of nanowires exhibits narrow resonances that are sensitive to changes in the surrounding of the nanowires. Subnanometer changes in the radius of the nanowires result in significant shifts of the reflection contrast. The reflection contrast peak is shifted by shells of SiO_2 with different thicknesses. We find that a shell with a thickness of only ~ 10 nm shifts the reflection contrast by $\sim 1°$. By fitting the reflection contrast measurement using the Jones calculus and Maxwell-Garnett effective medium theory, the thickness of the shell is determined with a high accuracy. The high sensitivity of the reflection contrast to changes in their surrounding medium renders ensembles of nanowires a promising material for sensing applications.

Acknowledgments

We thank G. Immink for the growth of the nanowires, E. Evens and R. van de Laar for technical assistance, F. Holthuysen for SEM analysis, M. Boamfa for useful discussions, and M. A. Verheijen for TEM analysis. This work is part of the research program of the "Stichting voor Fundamenteel Onderzoek der Materie (FOM)", which is financially supported by the "Nederlandse organisatie voor Wetenschappelijk Onderzoek (NWO)" and is part of an industrial partnership program between Philips and FOM.

Table 1. Evaporation times of the SiO_2 shell and resulting shell thicknesses.

Sample	Evaporation time [s]	Shell Thickness [nm]
I	0	0
II	4	10.3 ±1.3
III	8	16.7 ±2
IV	15	18.6 ±1.1
V	20	29.3 ±4.7

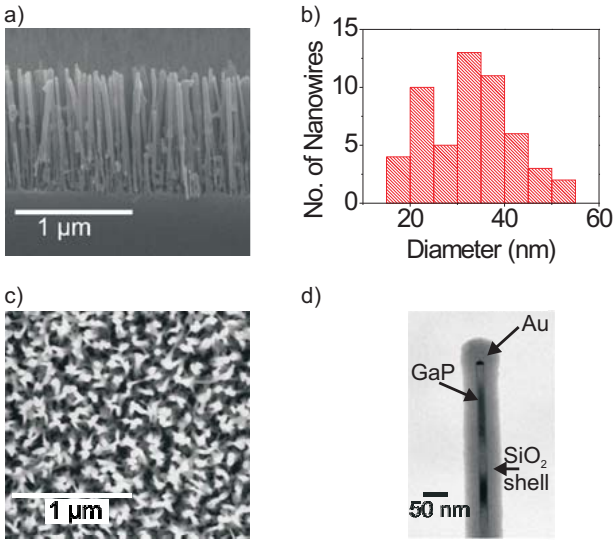

Figure 1. a) Cross-sectional SEM image of GaP nanowires on a GaP substrate (sample I in Table 1), b) histogram of the diameter distribution of the nanowires, c) top-view SEM image of the same sample, and d) TEM image of a nanowire covered with a 28 ± 2 nm thin shell of SiO_2. The gold catalyst particle, the GaP nanowire and the SiO_2 shell are marked.

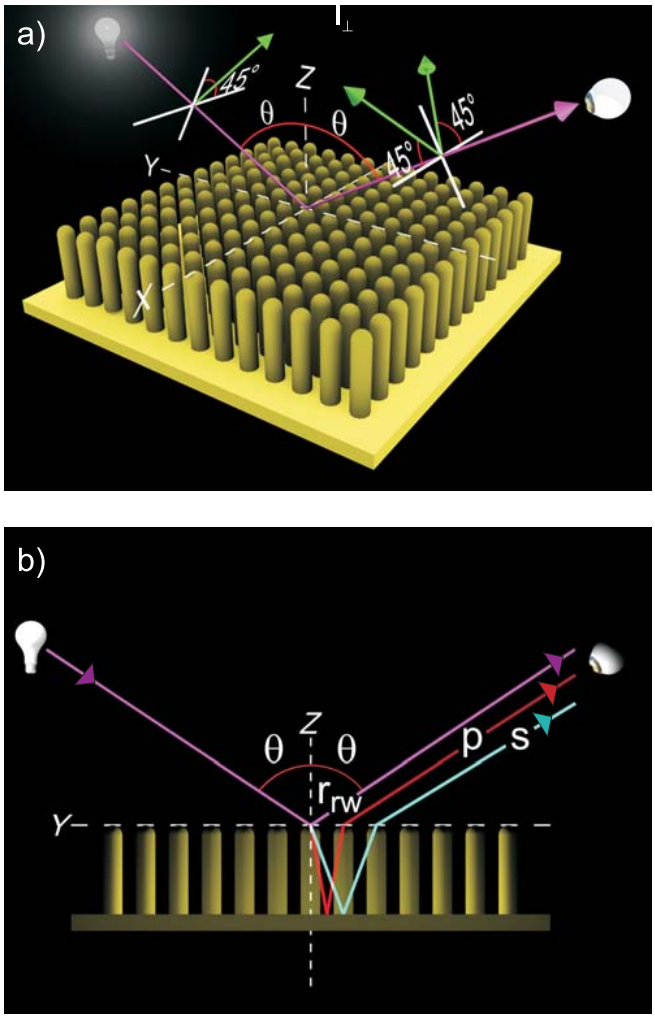

Figure 2. a) Schematic representation of the experimental setup. Light with the electric field vector oriented at 45° with respect to the plane of reflection is incident on the nanowire layer. The reflected light is measured with the analyzer set crossed and parallel to the incident polarization. The angle of incidence θ is varied in the experiment. b) Optical path of light beams reflected from and refracted into the nanowire layer. The incident light is partly reflected at the air-nanowire interface (magenta line). The fraction of light that enters the nanowire layer diffracts differently, depending on polarization: Light with the electric field component perpendicular to the nanowire elongation travels as a s-polarized wave in the layer (cyan line), while light with the electric field component parallel to the nanowire elongation travels as a p-polarized wave (red line). The s-polarized wave refracts into the nanowire layer according to the refractive index n_{s}, while the p-polarized wave is refracted according to n_{p}.

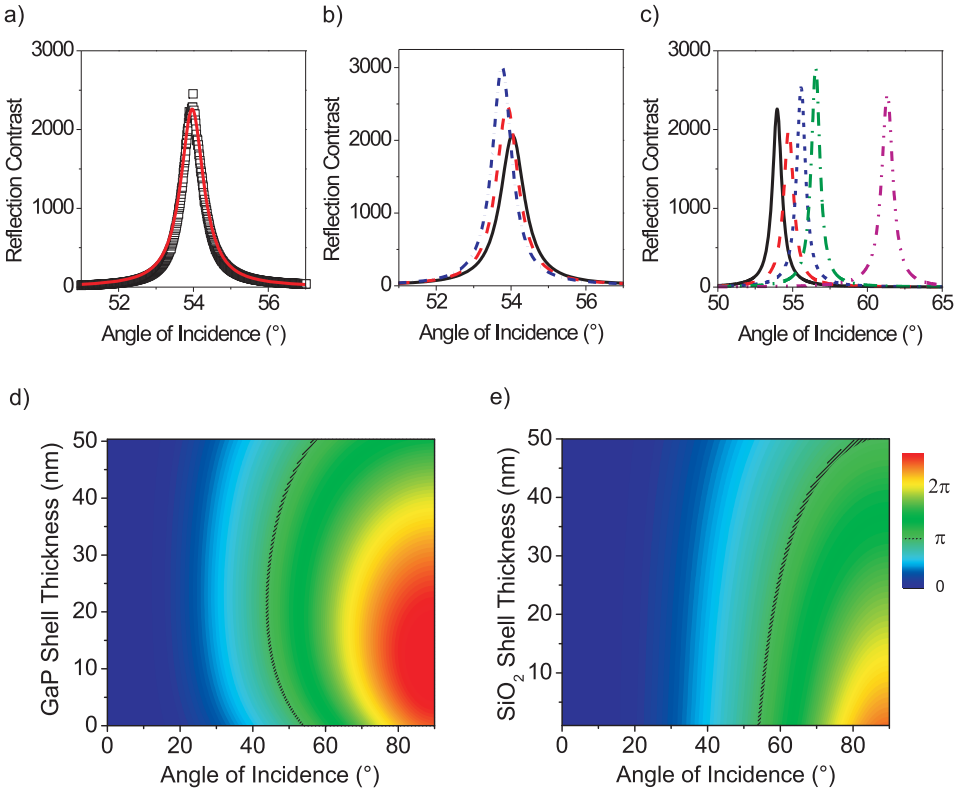

Figure 3. a) Measured (black squares) and calculated (red curve) reflection contrast of sample I (see Table 1) as a function of the angle of incidence. For the calculations, we consider a radius of the nanowires r_c = 19.65 nm, an average distance between nanowires of d_{nw} = 160 nm, and a nanowire layer thickness of 1 μm. b) Calculation of the reflection contrast for different nanowire radii r_c = 19.6 nm (black solid curve), 19.7 nm (red dashed curve), and 19.8 nm (blue dash-dotted curve). c) Calculated reflection contrast at λ = 532 nm of a layer of GaP nanowires without shell (black solid curve) and nanowires covered with a SiO_2 shell of 5 nm (red long-dashed curve), 10 nm (blue short-dashed curve), 15 nm (olive dash-dotted curve), and 30 nm (magenta dash-dot-dotted curve). The thickness of the nanowire layer is 1 μm and the radius of the nanowires and the average distance is r_c = 19.65 nm and d_{nw} = 160 nm, respectively. d) Calculation of the phase shift of light passing through a layer of GaP nanowires with a thickness of 1 μm, a radius of 19.65 nm and increasing GaP shell thickness as a function of angle of incidence. The black curve marks a phase shift of π. This phase shift corresponds to the maximum reflection contrast. e) Similar calculation as in d) but in this figure the thickness of a SiO_2 shell is varied.

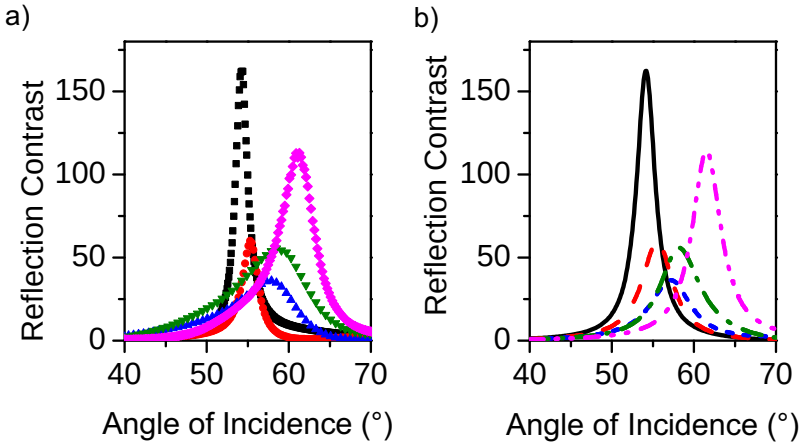

Figure 4. Measured reflection contrast of sample I (black squares), II (red circles), III (blue up-triangles), IV (olive down-triangles) and V (magenta diamonds) as a function of the angle of incidence and b) calculations of the reflection contrast for nanowires without shell (black solid curve) and shell thicknesses of 9 nm (red short-dashed curve), 18 nm (blue long-dashed curve), 19.7 nm (olive dash-dotted curve), and 30 nm (magenta dash-dot-dotted curve) for a 1 μm thick nanowire layer with a nanowire radius of $r_{\mathrm{c}} = 19.4$ nm and an average nanowire separation of $d_{\mathrm{nw}} = 160$ nm.

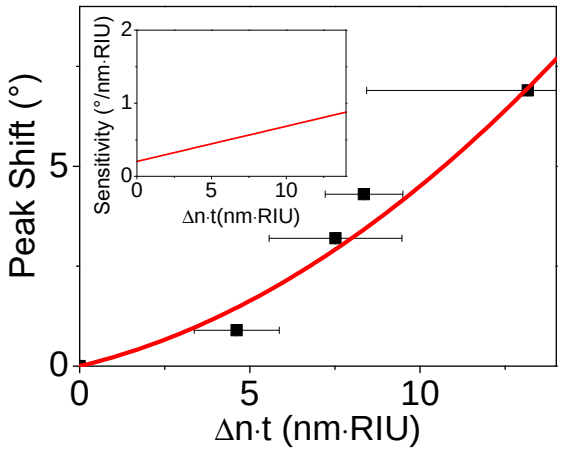

Figure 5. a) Measured shift of the peak in reflection contrast as a function of the product of the SiO_2 thickness, t, and the difference in refractive index Δn, between the shell and the surrounding medium, (black squares) determined from samples I-V and calculated peak shift of the reflection contrast (red curve). The peak shift is determined from the calculation shown in Figure 3c. The inset shows the sensitivity as a function of $\Delta n \cdot t$ determined from the calculation.

Appendix

Appendix A.1. Calculations based on Maxwell-Garnett effective medium theory and Jones calculus

The refractive index of s-polarized light n_s, which equals the ordinary refractive index n_o, is calculated using the Maxwell-Garnett effective medium theory for core-shell cylinders, as described in Ref. 17

$$n_\mathrm{s} = n_\mathrm{o} = \left[1 - \frac{2f_\mathrm{cs}}{\gamma_1 + f_\mathrm{cs}}\right]^{\frac{1}{2}}, \tag{A.1}$$

with

$$\gamma_1 = \frac{r_\mathrm{c}^2(\epsilon_\mathrm{s} - \epsilon_\mathrm{c})(\epsilon_\mathrm{d} - \epsilon_\mathrm{s}) + r_\mathrm{s}^2(\epsilon_\mathrm{s} + \epsilon_\mathrm{c})(\epsilon_\mathrm{d} + \epsilon_\mathrm{s})}{r_\mathrm{c}^2(\epsilon_\mathrm{s} - \epsilon_\mathrm{c})(\epsilon_\mathrm{d} + \epsilon_\mathrm{s}) + r_\mathrm{s}^2(\epsilon_\mathrm{s} + \epsilon_\mathrm{c})(\epsilon_\mathrm{d} - \epsilon_\mathrm{s})}, \tag{A.2}$$

and with r_c being the radius and ϵ_c the permittivity of the core, r_s the radius of the core-shell nanowire and ϵ_s the permittivity of the shell, surrounded by a dielectric with the permittivity ϵ_d. The filling fraction of the coated nanowires is calculated using $f_\mathrm{cs} = \pi r_\mathrm{s}^2/d_\mathrm{nw}^2$ with d_nw the distance between the midpoints of two nanowires. The extraordinary refractive index is calculated as the geometrical average of the three media [30]

$$n_\mathrm{e} = \sqrt{f_\mathrm{c}\epsilon_\mathrm{c} + f_\mathrm{s}\epsilon_\mathrm{s} + (1 - f_\mathrm{c} - f_\mathrm{s})\epsilon_\mathrm{d}}, \tag{A.3}$$

with $f_\mathrm{c} = \pi r_\mathrm{c}^2/d_\mathrm{nw}^2$ and $f_\mathrm{s} = f_\mathrm{cs} - f_\mathrm{c}$.

From the ordinary, n_o, and the extraordinary, n_e, refractive indices, the refractive index for p-polarized light can be calculated with [26]

$$n_\mathrm{p} = \sqrt{n_\mathrm{o}^2 + \frac{n_\mathrm{e}^2 - n_\mathrm{o}^2}{n_\mathrm{e}^2} \cdot \sin^2\theta}. \tag{A.4}$$

The reflection from a layer of nanowires can be modeled with the Jones calculus for a three layer system consisting of air, nanowires and the substrate according to Figure 2b [18]. The Jones calculus is based on Jones vectors describing the polarization of the incident light and of the analyzer, the transmission and reflection coefficients at the interfaces, and the phase changes in air and in the nanowire layer.

References

[1] Borgström M T, Immink G, Ketelaars B, Algra R and Bakkers E P A M 2007 *Nature Nanotech.* **2** 541

[2] Mohammad S N 2008 *Nano Lett.* **8** 1532–1538

[3] Gabrielli L, Cardenas J, Poitras C and Lipson M 2009 *Nature Photonics* **3** 461 – 463

[4] Pierret A, Hocevar M, Diedenhofen S L, Algra R E, Vlieg E, Timmering E C, Verschuuren M A, Immink G W G, Verheijen M A and Bakkers E P A M 2010 *Nanotechnolgy* **21** 065305

[5] Wacaser B A, Dick K A, Johansson J, Borgström M T, Deppert K and Samuelson L 2009 *Adv. Mat.* **21** 153–165

[6] Haraguchi K, Katsuyama T, Hiruma K and Ogawa K 1992 *Appl. Phys. Lett.* **60** 745–747

[7] Tian B, Zheng X, Kempa T J, Fang Y, Yu N, Yu G, Huang J and Lieber C M 2007 *Nature* **449** 885–890

[8] Lee Y J, Ruby D S, Peters D W, McKenzie B B and Hsu J W P 2008 *Nano Lett.* **8** 1501

[9] Diedenhofen S L, Vecchi G, Algra R E, Hartsuiker A, Muskens O L, Immink G, Bakkers E P A M, Vos W L and Gómez Rivas J 2009 *Adv. Mat.* **21** 973–978

[10] Tsakalakos L, Balch J, Fronheiser J, Korevaar B A, Sulima O and Rand J 2007 *Appl. Phys. Lett.* **91** 233117

[11] Goodey A P, Eichfeld S M, Lew K K, Redwing J M and Mallouk T E 2007 *J. Am. Chem. Soc.* **129** 12344–12345

[12] Wang J, Gudiksen M S, Duan X, Cui Y and Lieber C M 2001 *Science* **293** 1455–1457

[13] Cao L, Fan P, Barnard E S, Brown A M and Brongersma M L 2010 *Nano Lett.* **10** 2649–2654 (*Preprint* `http://pubs.acs.org/doi/pdf/10.1021/nl1013794`)

[14] Muskens O L, Borgström M T, Bakkers E P A M and Gómez Rivas J 2006 *Appl. Phys. Lett.* **89** 233117

[15] Gross E, Kovalev D, Künzner N, Timoshenko V Y, Diener J and Koch F 2001 *J. Appl. Phys.* **90** 3529–3532

[16] Muskens O L, Diedenhofen S L, van Weert M H M, Borgström M T, Bakkers E P A M and Gómez Rivas J 2008 *Adv. Func. Mat.* **18** 1039

[17] Nicorovici N A, McKenzie D R and McPhedran R C 1995 *Optics Comm.* **117** 151–169

[18] Hodgkinson I J and Wu Q H 1997 *Birefringent Thin Films and Polarizing Elements* (World Scientific)

[19] Stefano L D, Rendina I, Moretti L, Tundo S and Rossi A M 2004 *Appl. Opt.* **43** 167–172

[20] Künzner N, Gross E, Kovalev D, Timoshenko V Y and Wallacher D 2003 *J. Appl. Phys.* **94** 4913–4917

[21] Lin V S Y, Motesharei K, Dancil K P S, Sailor M J and Ghadiri M R 1997 *Science* **278** 840–843

[22] Dancil K P S, Greiner D P and Sailor M J 1999 *J. Am. Chem. Soc.* **121** 7925–7930

[23] Létant S E and Sailor M J 2001 *Adv. Mat.* **13** 335–338

[24] Wagner R S and Ellis W C 1964 *Appl. Phys. Lett.* **4** 89–90

[25] Born M and Wolf E 1997 *Principles of Optics* 6th ed (Cambridge University Press)

[26] Oton C J, Gaburro Z, Ghulinyan M, Pancheri L, Bettoti P, Negro L D and Pavesi L 2002 *Appl. Phys. Lett.* **81** 4919–4921

[27] Diedenhofen S L and Gómez Rivas J 2010 *Semicond. Sci. Technol.* **25** 024008

[28] Palik E (ed) 1998 *Handbook of optical constants of solids* (Academic Press)

[29] Schulz B, Chan D, Bäckström J and Rübhausen M 2004 *Thin Solid Films* **455-456** 731–734

[30] Kirchner A, Busch K and Soukoulis C M 1998 *Phys. Rev. B* **57** 277–288